Available online at www.sciencedirect.com
SCIENCE DIRECT
Polymer 47 (2006) 5513–5522
polymer
www.elsevier.com/locate/polymer

Morphology and growth of a hydroxybutyrate oligomer with 24 repeat units

S.J. Organ [a,*], J. Li [a,b], A.E. Terry [c], P.J. Barham [b]

[a] Department of Materials Engineering, The Open University, Walton Hall, Milton Keynes MK7 6AA, UK
[b] H H Wills Physics Laboratory, University of Bristol, Tyndall Avenue, Bristol BS8 1TL, UK
[c] Department of Chemical Engineering, Eindhoven University of Technology, P.O. Box 513, 5600MB Eindhoven, The Netherlands

Received 14 February 2005; accepted 27 February 2005
Available online 18 May 2006

Abstract

The crystallization behaviour of an oligomer of hydroxybutyrate containing 24 repeat units has been studied over a wide range of temperature using optical microscopy to measure growth rates and observe morphologies and small angle X-ray scattering to measure crystal thicknesses. Crystals grew with a wide range of thicknesses between $E/2$ and E, where E is the extended chain length. Preferred crystal thicknesses corresponded to simple fractions of E, which result in a relatively higher proportion of chain folds in the surface. Growth rates peaked at 75 °C and were unusually scattered at temperatures corresponding to a change in preferred chain conformation. Spherulites grown at the lower temperatures were banded: as the crystallization temperature was increased the banding disappeared, the shapes of the spherulites became less regular, and a coarser texture associated with reduced branching developed.

Keywords: Hydroxybutyrate oligomers; Spherulite morphologies; Growth rates

1. Introduction

One of the major thrusts of David Bassett's extensive research contribution has been the elucidation, by careful, detailed, and often beautiful electron microscopic examination, of the nature and origin of spherulites [1]. Among many aspects of this work, the use of monodisperse long *n*-alkanes of precise length has helped to test the validity of different proposed growth mechanisms [2–4]. It therefore seemed appropriate for this special issue to report on some of our latest work on a hydroxybutyrate oligomer, which produces particularly large and well-defined spherulites over a wide range of growth conditions, and which shows some fundamental differences in behaviour from the *n*-alkanes.

Oligomer chains long enough to fold, yet short enough to obtain in a pure form, provide useful model systems for studying growth, annealing and melting in materials that crystallize via chain folding and help to advance our understanding of more complex polymeric behaviour. Much of the interest has been concentrated on long *n*-alkanes and this work, together with key results from other systems has been summarised in a recent review [5].

In recent series of papers [6–8], preliminary findings were reported from a series of hydroxybutyrate (HB) oligomers, which are short chain analogues of the polymer polyhydroxybutyrate (PHB). Most of the work was based on oligomers containing 24 or 32 repeat units (to be referred to as 24-mer and 32-mer), some of which were capped with a protecting benzyl end-group. The formula of the unprotected 24-mer, which is the subject of this paper, is given below.

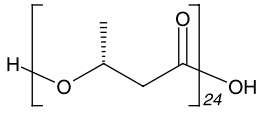

Under most conditions crystals of both the 24-mer and the 32-mer grew from the melt in a form in which the chains were folded. In contrast to the *n*-alkanes, the thickness of the folded chain forms did not always correspond to an exact integer fraction of the extended chain length. The fairly limited thickness data available displayed a wider range of possible crystal thicknesses and suggested a particular preference for crystals with a thickness close to two thirds of the extended chain length [6]. On heating, the folded chains within the crystals became extended: this was demonstrated clearly by simultaneous in situ measurements of crystallinity (from wide

* Corresponding author.
E-mail address: s.j.organ@open.ac.uk (S.J. Organ).

0032-3861/$ - see front matter © 2006 Elsevier Ltd. All rights reserved.
doi:10.1016/j.polymer.2005.02.132

angle X-ray scattering) and crystal thickness (from small angle X-ray scattering) during heating [8].

Crystals of 32-mer were also grown from solution in propylene carbonate [7]. A transition in behaviour was observed at around 36 °C. Crystals grown below this temperature thickened when heated: crystals grown above it did not. The transition could therefore be associated with a change from folded chain crystals (in unspecified conformation) below 36 °C and extended chain crystals above. Crystallization rates were measured from the increase in intensity of the main (020) diffraction peak as a function of time. In the region where the transition from folded to extended chain growth occurred there was some evidence of a slight discontinuity in the crystallization rate vs crystallization temperature curve, but this was much less pronounced than the very clear minimum in crystallization rate seen in solution grown *n*-alkanes when the chain conformation changes from folded to extended [e.g. 9,10].

In this paper, we present growth rate measurements from melt-crystallized HB 24-mer. This oligomer grows from the melt in the form of large, well-defined spherulites, which are clearly visible in an optical microscope. The use of crossed polars enhances contrast and provides additional morphological information to complement the growth rate data. Finally, small angle X-ray measurements of representative samples allow us to correlate the growth rate data with the associated crystal thicknesses.

Bassett et al. have noted that the appearance of polyethylene and alkane spherulites changes with the temperature at which they are formed [1]. The banding generally becomes more widely spaced, and less regular, as the crystallization temperature is increased and is often completely absent when spherulites are grown at the highest temperatures. Furthermore, the overall shape of the spherulites, grown in thin films, changes from perfectly circular forms at the lower crystallization temperatures to less regular shapes at the higher temperatures. We report here very similar observations from the HB oligomer system.

2. Experimental

The 24-mer used in these studies was kindly provided by Professor Seebach of ETH Zurich and was synthesised using the segment-coupling method described in Ref. [11].

Crystal growth rates were measured from direct observations of the growth of spherulites in an optical microscope, under crossed polars. In most cases small samples of oligomer were melted between two glass cover slips on a Linkam hotstage: typical conditions for melting were 0.5 min at 170 °C. The samples were then cooled at 80 °C min^{-1} until they reached the required crystallization temperature, T_c. At this point, a timer was started and digital photographs were taken at appropriate intervals as spherulites nucleated and grew at constant temperature, using a Pixelink digital camera attached to the microscope. In order to extend the range of accessible crystallization temperatures it was often advantageous to use two hot stages—melting the sample on one and then rapidly transferring to a second, pre-set to the crystallization temperature—in order to avoid complete crystallization during cooling. Where possible, measurements were repeated using both methods; these confirmed that the experimental set-up used did not affect the result obtained.

Growth rates were calculated from the increase in spherulite radius, r, with time, t, which showed a linear relationship. Each sample was used for several measurements, until degradation (indicated by a reduction in melting temperature) became apparent.

Crystal thicknesses were measured by small angle X-ray scattering, either at the University of Bristol using a Bruker AXS Hi-Star SAXS ($\lambda = 0.1541$ nm) or at ESRF Grenoble using the high brilliance beamline ID2 ($\lambda = 0.0995$ nm): more details of the experimental set-up are given in Ref. [6]. Most samples were crystallized isothermally as described above and then subsequently scraped into 1.5 mm diameter Lindemann tubes for exposure to the X-ray beam at room temperature. In a few cases, measurements were made at higher temperatures either during in situ crystallization or after heating; these are distinguished in the results section. Crystallization times were kept as short as possible (typically a few minutes) to allow the majority of the sample to crystallize, while minimising the opportunity for isothermal thickening. Typical exposure times were a few hours in Bristol, 2–3 s at ESRF. Thickness values were calculated from the peak positions using Bragg's law, after the usual corrections for intensity had been applied.

3. Results

Fig. 1 shows examples of spherulites growing at two different temperatures: the different morphologies will be discussed later. A typical set of data from which a growth rate was calculated is shown in Fig. 2. Each set of points represents a different spherulite from the same sample or, where very few spherulites were obtained, a different cross section from the same spherulite. In the few cases where the crystals were not circular (as in Fig. 1(b)) the longest dimension was measured. The spherulite radius increases in a linear fashion as seen in Fig. 2: a growth rate was calculated from the gradient of each line and the average found. The values obtained from the individual crystals within the same sample differ by less than 1%. It is obvious from Fig. 2 that the crystals have all nucleated at around the same time—in this case close to $t_c = 0$. This was often (though not exclusively) found to be the case, and suggests that the nucleation is primarily heterogeneous. At the lower crystallization temperatures (and particularly where only one hot stage was used) crystals often started to grow before T_c was reached (i.e. before $t_c = 0$): however, comparison of results from different crystals and different samples confirms that this did not affect the subsequent rate of growth at T_c.

Fig. 3 plots growth rate as a function of crystallization temperature over the range 40–120 °C. Each point is the average of several measurements taken from different crystals within the same sample, as described above. Where more than one point is plotted for a particular temperature these refer to independent measurements from different samples. The growth

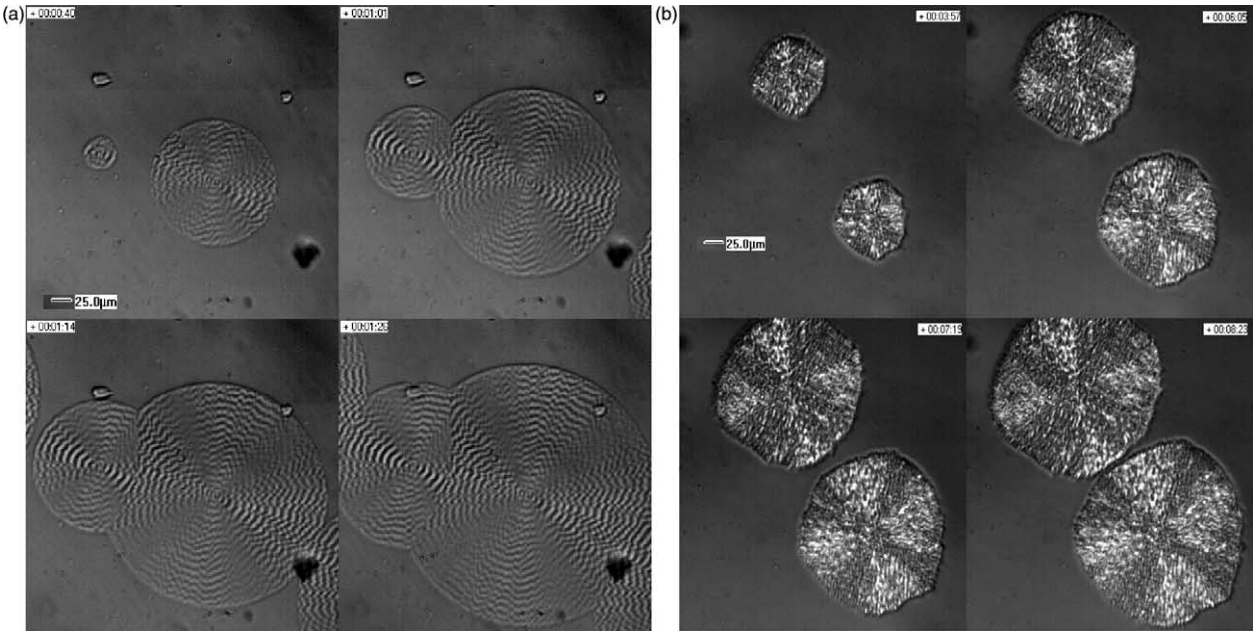

Fig. 1. Examples of spherulites of 24-mer growing at (a) 63 °C (b) 99 °C. Optical micrographs, crossed polars. The 25.0 μm marker applies to all figures. Crystallization times are as shown.

rate curve shown in Fig. 3 has the distinctive form expected (but rarely fully accessible experimentally) from a crystallisable polymer. Similar curves have been obtained, for instance, from PHB and its co-polymers [12,13] but we believe this to be the most complete curve obtained to date from an oligomer system.

At the high temperature end of the curve the growth rate rises as the crystallization temperature falls, due to the increase in thermodynamic driving force with supercooling. As the temperature is reduced further the growth rate passes through a maximum and then falls. This is due to reduced mobility of the chains as the viscosity of the melt increases: the crystallization rate is restricted to the rate at which chains can diffuse to the growing surface, and this falls with temperature. Apart from the very obvious peak in growth rate at $T_c = 75$ °C there are two regions of the curve, at around 85 and 100 °C, where the data is particularly scattered. We will return to consider these later.

A few examples of growing spherulites were shown in Fig. 1. Further examples of the morphology obtained over a wider range of temperatures are shown in Fig. 4. These pictures have been chosen to illustrate spherulites of similar size to each other (the 25 μm marker shown in Fig. 4(a) applies to all the pictures) but note that the corresponding crystallization times vary considerably, reflecting variations in both growth and nucleation rates. No attempt has been made to quantify nucleation rates, since most nucleation appears to be heterogeneous, but a general trend towards higher nucleation rates (and shorter incubation times) was observed as T_c was reduced.

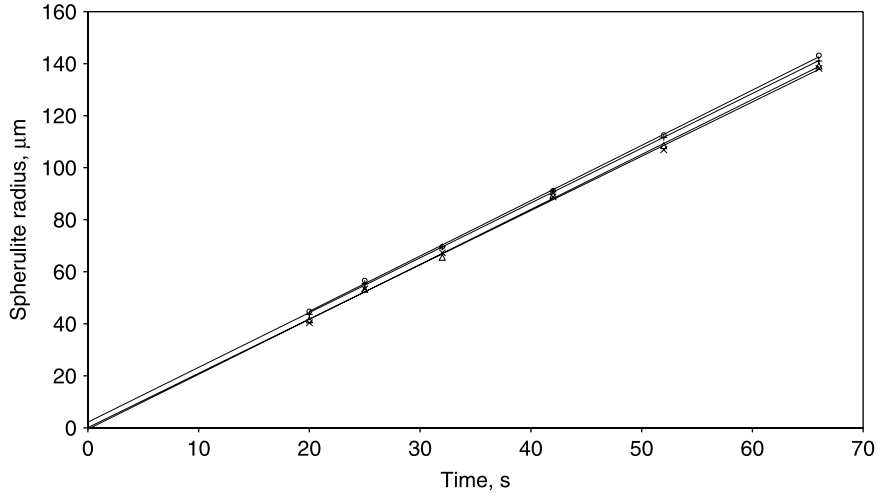

Fig. 2. Spherulite radius as a function of time for four 24-mer spherulites growing at $T_c = 82$ °C.

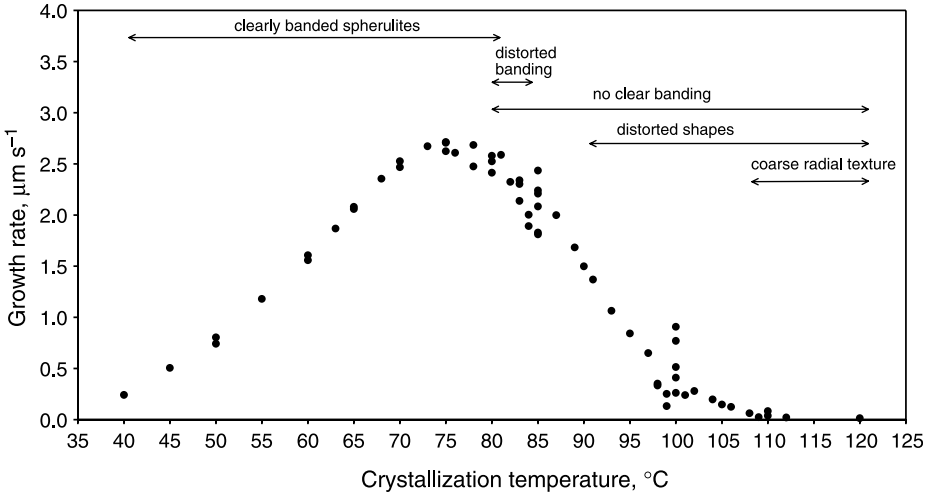

Fig. 3. Growth rate as a function of crystallization temperature for the 24-mer.

The general types of morphology observed, and the temperature ranges over which they occur, are indicated on Fig. 3. At crystallization temperatures of 80 °C and below the spherulites are particularly distinctive, showing very clear and often extremely regular banding. Examples are shown in Fig. 4(a)–(c). The band spacing did not vary significantly with temperature, falling in the range 4–8 μm for the vast majority of samples. This is remarkably similar to the essentially constant band spacing observed in PHB over a similar temperature range [12,14]: Fig. 5 shows band spacing as a function of crystallization temperature for our samples and includes PHB data from Ref. [14] for comparison. The sharp rise in band spacing seen at around 100 °C in PHB was not observed in our samples: instead, the regular banding begins to break down as the crystallization temperature is raised from 80 to 85 °C. Some crystals grown in this temperature range displayed a distorted band structure, such as that shown in Fig. 4(d), while in others no banding was visible at all. Above 85 °C no clear banding was ever observed.

Significant differences in birefringence occurred in the non-banded crystals. Fig. 4(e) shows an example of a crystal grown at 90 °C, which displays very little contrast—indeed even the maltese cross is absent—while the crystal grown at 98 °C shown in Fig. 4(f) is much brighter. The variations in birefringence showed no clear correlation with crystallization temperature, sample, or experimental method (use of one or two hot-stages).

At temperatures above 90 °C the perfectly spherical shapes began to look distorted and the outer edges less well defined. This is most apparent in Fig. 4(h) where the crystals are distinctly asymmetrical. These entities are reminiscent of the structures described as hedrites, or axialites, sometimes observed in polymeric systems at high crystallization temps [15–17] and believed to arise from large clumps of single crystals. A further, more subtle, change in morphology occurs at the highest temperatures, where a coarse radial texture starts to appear. This is most clearly illustrated in Fig. 4(j).

The crystal thicknesses measured from samples grown over the same range of temperature are shown in Fig. 6, with the different experimental methods distinguished. A few data points previously reported in Ref. [6] from the same material are included for completeness. The 'ESRF, crystallization in situ' data were recorded at the crystallization temperature and a correction for thermal expansion has been applied using data from Ref. [8]. Where two such points are shown at the same temperature they refer to different crystallization times and this will be explained in Section 4. All the other results were measured at room temperature with the exception of the 'previous results' point at 120 °C, which refers to material that has thickened on heating and for which no reference is available. Some samples showed a very small secondary population of crystals of a distinctly different thickness: these crystals are likely to have grown on quenching, at a lower temperature than the initial crystallization.

4. Discussion

Our results provide complementary sets of data describing crystal growth rates, morphologies and thicknesses. To examine the possible links between them we will start by considering the different chain conformations that might be involved.

4.1. Chain conformations in HB 24-mer

In a previous paper [8], we have shown that crystals of 24-mer grown at room temperature contain folded chains which, when heated to around 140 °C, unfold to produced extended chain crystals. The thicknesses of these crystals, before and after heating, have been included in Fig. 6 (labelled 'previous results'). In that case, the folded chain form had a thickness close to half of the extended chain length ($E/2$), implying that the chains were folded exactly in half. Other thickness measurements from both 24-mer and 32-mer suggested that a crystal form with thickness close to 2/3 of the extended chain length ($2/3E$) was also common. This is in contrast to results from long *n*-alkanes where stable crystal thicknesses have been found to correspond only to integer fractions of the extended

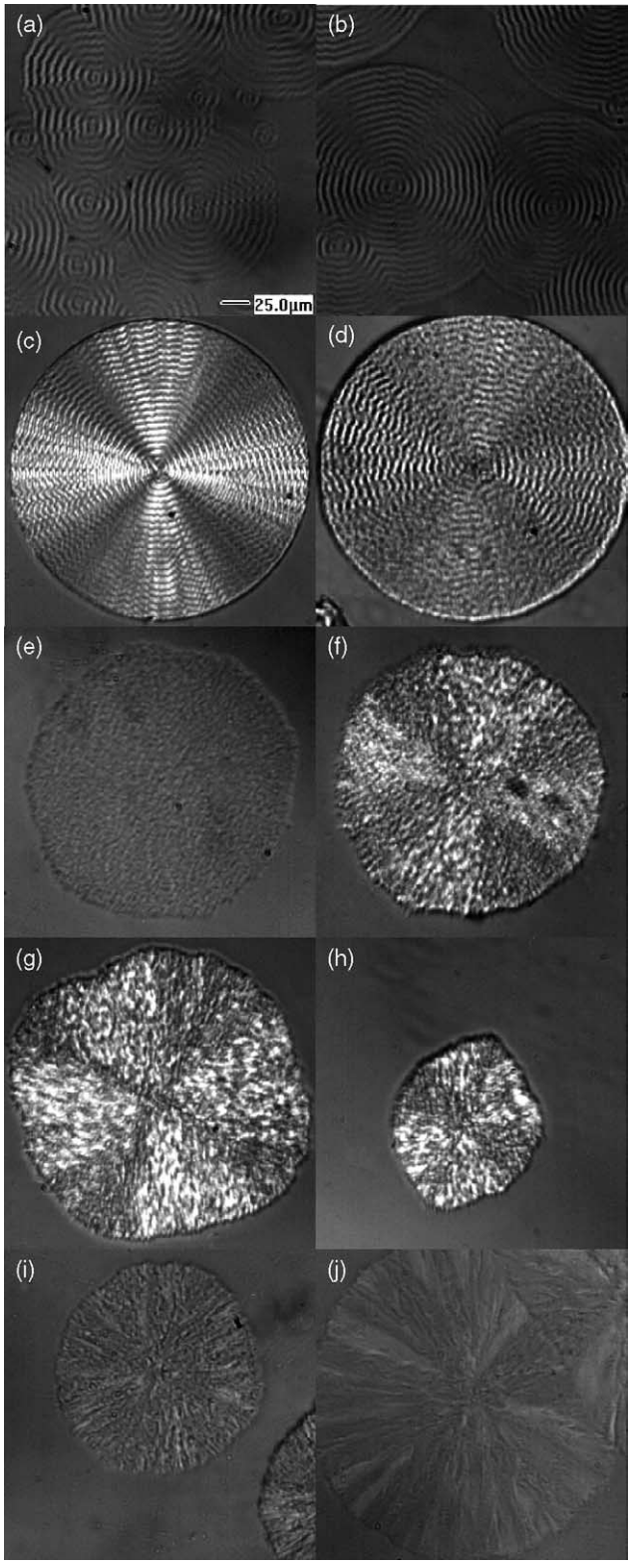

Fig. 4. Examples of spherulite morphology obtained from 24-mer grown at different temperatures (T_c). Crystallization times (t_c) have been chosen so that the spherulites are of similar size. The 25 µm marker applies to all the frames. (a) $T_c = 50$ °C, $t_c = 1$ min 45 s; (b) $T_c = 55$ °C , $t_c = 1$ min 37 s; (c) $T_c = 75$ °C, $t_c = 1$ min 11 s; (d) $T_c = 85$ °C, $t_c = 1$ min 27 s; (e) $T_c = 90$ °C, $t_c = 1$ min 6 s; (f) $T_c = 98$ °C , $t_c = 6$ min 46 s; (g) $T_c = 100$ °C , $t_c = 13$ min 41 s; (h) $T_c = 101$ °C, $t_c = 12$ min 32 s; (i) $T_c = 112$ °C, $t_c = 58$ min 18 s; (j) $T_c = 120$ °C, $t_c = 3$ h 14 min.

chain length ($E/2$, $E/3$, etc). It was suggested that, in the HB oligomers, hydrogen bonding between chain ends could effectively link chains together into longer units, making a wider range of chain conformations possible.

The current, more comprehensive, results from the 24-mer shown in Fig. 6 demonstrate clearly that a wide range of thicknesses can be obtained between the values $E/2$ and E, although the relationship between crystal thickness and crystallization temperature is not straightforward. We know from wide-angle X-ray scattering results that the samples are highly crystalline [6]. Assuming a simple model in which the oligomer chains are linked together by hydrogen bonds to create pseudo-polymers, which crystallize via adjacent re-entry at the crystal surface, a series of discrete values of crystal thickness are possible corresponding approximately to the length of n repeat units where n lies between 12 and 24. The length of each repeat unit corresponds to half the c spacing in the unit cell, i.e. 0.3 nm [12].

At the lowest crystallization temperatures, we obtain a value of thickness close to $E/2$. A small proportion of crystals with this thickness were also detected in samples grown at much higher temperatures, consistent with some secondary crystallization on quenching to room temperature. Once folded crystals of 24-mer begin to melt at around 105 °C [8] so it is extremely unlikely that these crystals could have grown at the crystallization temperature. At the highest temperature of 120 °C we obtain a thickness very close to the extended chain length, both from primary crystallization and from folded chain crystals that have been heated subsequent to growth [8]. Between these extremes a range of values are obtained, but the points are clustered particularly around values corresponding approximately to chains with 16 and 18 repeat units.

The small plateau at a thickness corresponding to 16 repeat units confirms our earlier suggestion that a crystal thickness of $2/3E$ is a preferred value, although the preference is not strong. We argued that this thickness was energetically favoured because the arrangement of chains resulted in a relatively high proportion of chain ends on the crystal surface (and hence a lower surface energy). We can extend this model further by calculating the proportion of chain ends that would lie on the surface of a perfect crystal for each value of n between 12 and 24: this is shown on the chart in Fig. 7. Using this simple model, we see that chain conformations with 12 and 24 repeat units are particularly favourable (as expected) followed by 16 ($2/3E$), 18 ($3/4E$) and 20 ($5/6E$). The chain conformations corresponding to these values are sketched in Fig. 8.

The experimentally observed preference for crystals with thickness close to 16 and 18 monomer units is thus consistent with the prediction from our simple model for the most energetically favourable thicknesses. The actual measured thicknesses are slightly less than the exact fractional values, as would be expected due to the length of chain involved in the fold. A preference for a thickness corresponding to 20 repeat units is less clear, although crystals grown at 106 and 110 °C both yielded results quite close to this value.

The nominal beam size for both X-ray systems used is comparable at about 0.3 mm diameter, so that in these

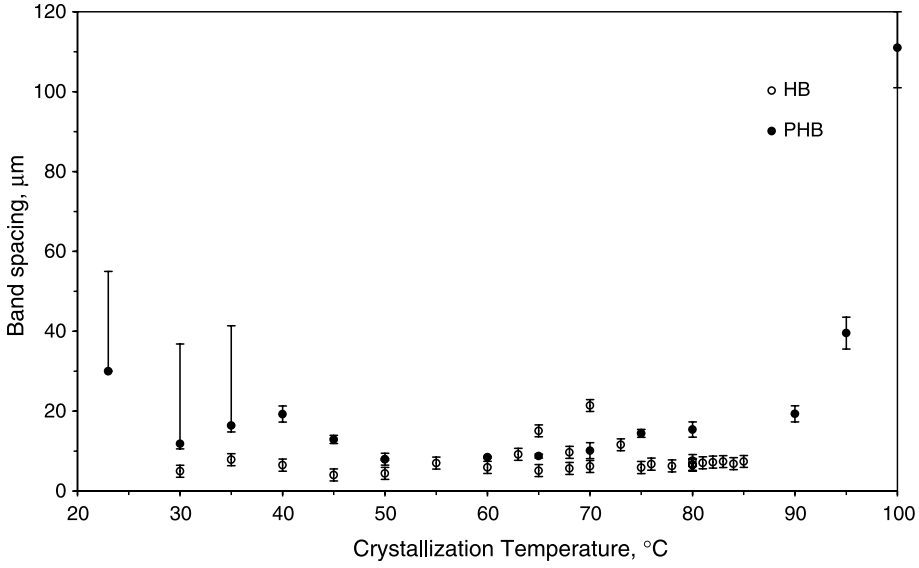

Fig. 5. Band spacing in spherulites of HB 24-mer and PHB (from Ref. [14]).

experiments we will generally be sampling several spherulites simultaneously. The two systems use different types of X-ray source, optics and detectors, which result in significantly better resolution in the ESRF system. If crystals are growing within the same sample with different, but similar, thicknesses this will be particularly difficult to resolve using the 'Bristol' set-up and we cannot rule out the possibility of mixed crystal populations in these samples.

A second complication is that crystals can, and do, thicken during growth. The pairs of points recorded in situ at ESRF at 85, 100 and 110 °C were each obtained during a single crystallization run, the lower point coming from the initial growth and the upper point taken after crystallization was complete. This is an aspect that requires further investigation and will form the subject of a subsequent publication. Apart from the points described above, crystallization times were relatively short; chosen to allow most of the sample to crystallize, while minimising the time available for annealing.

4.2. Crystal growth rates

The growth rate vs crystallization temperature curve in Fig. 3 reveals particularly scattered growth rate measurements at 85 and 100 °C. By comparison with Fig. 6, it is interesting to note that 85 °C corresponds to the point at which the crystal thickness changes from 16 to 18 monomer units and 100 °C marks the end of the temperature region where values close to 18 monomer units are favoured. At both these temperatures, a number of slightly different crystal thicknesses were measured. Since, each growth rate measurement corresponds to an individual spherulite, while the SAXS measurements are likely to encompass several different spherulites, it seems plausible

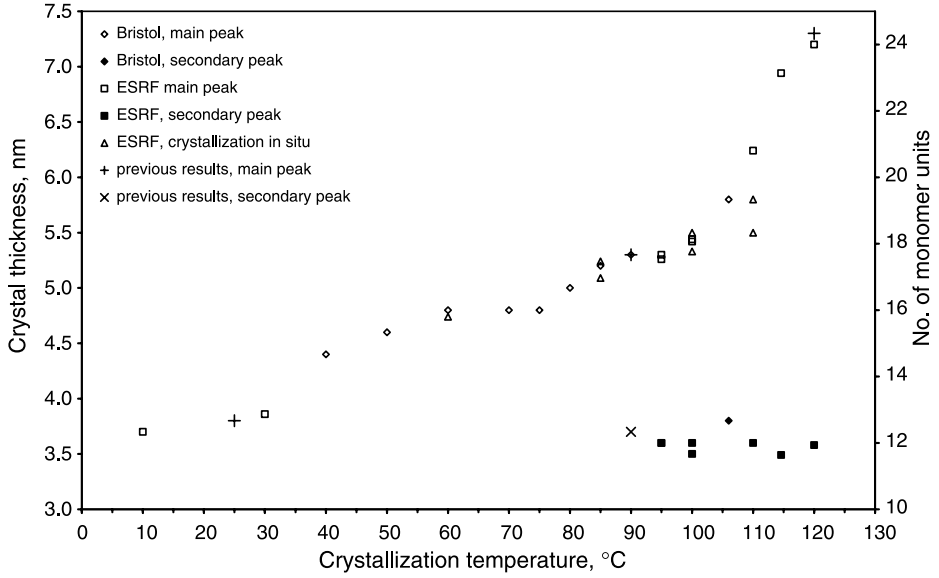

Fig. 6. Crystal thickness as a function of crystallization temperature. See text for details.

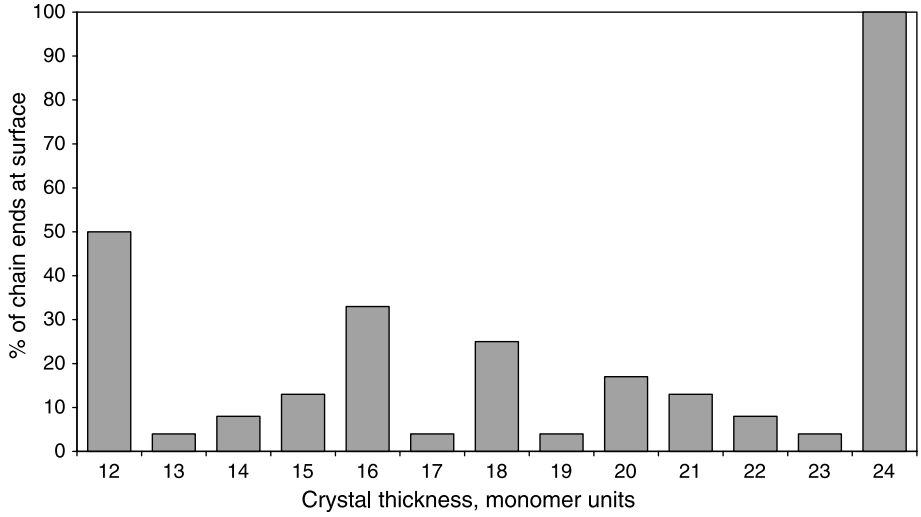

Fig. 7. Chart showing the percentage of chain ends in the crystal surface for different crystal thicknesses; see text for an explanation of the assumptions made.

that what we are seeing here is the result of competition between two similarly stable crystal forms. An individual spherulite might grow in either form, depending on the initial nucleation conditions, while the SAXS result would be skewed towards the thickness of the majority population.

We know that crystals with different thicknesses have different melting points; the thicker the crystal the higher the melting point. Similarly, the supercooling at which a crystal grows will depend not only on the temperature, but also upon the actual crystal form (thickness) in which it grows. This leads to an interesting phenomenon. At a higher crystallization temperature only a thick crystal can grow. As the temperature is reduced, so the supercooling for that crystal thickness increases and hence its crystallization rate also increases. Eventually the temperature falls below the melting point of a thinner crystal form, so it may start to grow. But the supercooling for that form is still low and it will only grow slowly; however, as the temperature falls further the growth rate increases and it can become the faster growing crystal, so it dominates.

In previous work on *n*-alkanes large changes in growth rate were seen near the temperatures at which the crystal growth changed between different integer folded forms. In many cases, these changes were so pronounced that the growth rate passed through a minimum at, or close to, the transition temperature [2,9]. At high temperatures only the thicker form is stable, then as the temperature is reduced it becomes possible for a thinner form to grow. The rate of growth of both forms increases with decreasing temperature, but they do not actually increase at the same rate so that at some temperature the thinner form can become the faster growing one. This on its own would lead to a graph of growth rate vs temperature with a number of branches, one for each thickness. In general, one would then expect the growth rate to follow the highest possible growth rate since the faster growing crystals would tend to dominate. Various explanations for the deviations from this behaviour with minima in growth rate at the transitions have been given, but essentially all are similar. If a thin crystal starts to form at the surface of a thicker one at a temperature where the thicker crystals still have a higher growth rate then growth is actually retarded, leading to a reduction in growth rate.

The data shown here do show some apparent discontinuities in growth rate, particularly at temperatures around 100 and 85 °C, but there is no pronounced minimum as in the *n*-alkanes. However, the small angle X-ray data shown in Fig. 6 suggest that there may well be changes in the thicknesses of the growing crystals near these temperatures; from 16 to 18 repeat units at around 85 °C and from 18 to 20 repeats near 100 °C.

Unfortunately, we do not have direct measurements of the thicknesses of crystals on which the growth rate measurements were made. However, we can look in greater detail at the variation of growth rate with temperature in an attempt to see whether there are differences that may be attributed to changes in crystal thickness. It is conventional to plot $\ln G$ against $1/T_c\Delta T$ and expect to see a linear graph, rather than the highly curved graph obtained when G is plotted against T_c as in Fig. 3 [18]. However, in our case we know that different crystals are growing with different thickness and at different supercoolings, so we can attempt a more general plot.

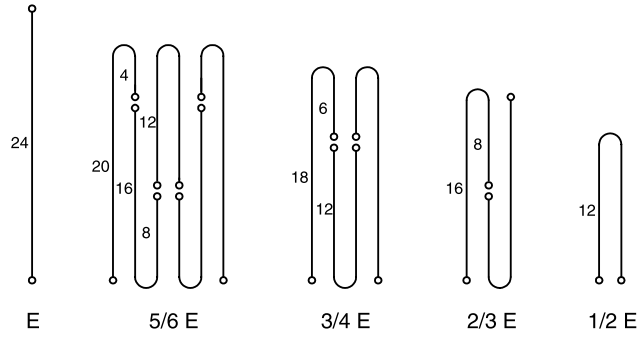

Fig. 8. A schematic drawing showing the favourable chain conformations corresponding to extended (*E*), 5/6*E*, 3/4*E*, 2/3*E* and 1/2*E* chain forms, ignoring the chain length involved in the folds for simplification. The circles represent the OH groups at the chain ends and the numbers indicate the number of monomer repeat units in each section.

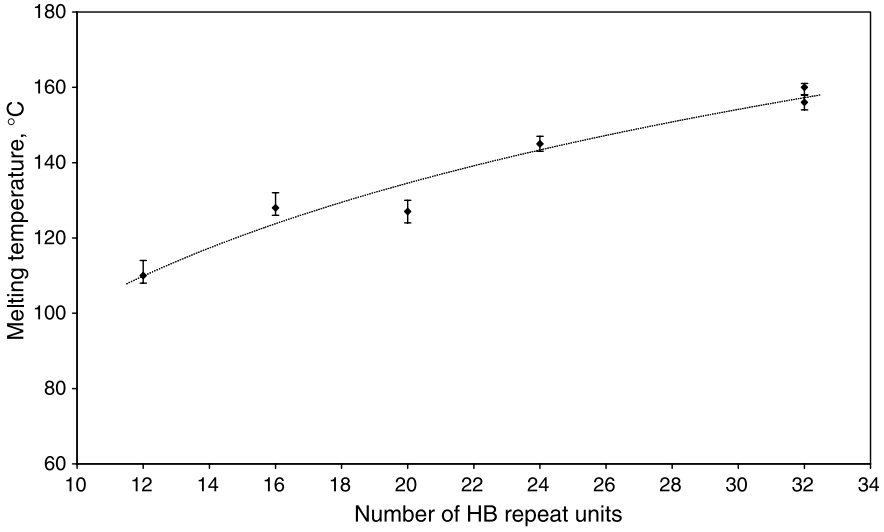

Fig. 9. Variation in melting temperature with crystal thickness, expressed in number of monomer units.

The melting temperatures corresponding to different chain lengths, from which the supercoolings are calculated, are taken from the graph of T_m vs n shown in Fig. 9. This is derived from data presented in Ref. [8] where the melting of different crystal forms of 24-mer and 32-mer of known thickness was observed directly using simultaneous SAXS and WAXS.

To construct the graph of $\ln G$ against $1/T_c\Delta T$ from the growth rate data in Fig. 3 we first selected a small subset of temperatures for which (by comparison with Fig. 6) we are reasonably confident of the crystal thickness. These were at 78, 90–95, 106–110 and 120 °C. The corresponding thicknesses are 16, 18, 20 and 24 monomer repeat units, respectively. These points are represented by the larger symbols on Fig. 10, and were used to generate the best-fit line shown on the graph.

We then plotted the remaining points, taking the range of possible thicknesses into account. For example, for crystallization between 79 and 89 °C we could have 16 or 18 repeat units, while between 97 and 105 °C we could have 18 or 20. These different possibilities are represented on Fig. 10 by the smaller symbols corresponding to each value of n. In most cases, it is clear that only one of the different possible thicknesses produces a data point near our expected line. In that case, we assume that the crystals actually grew with that thickness: those points are circled in Fig. 10.

Of course, this procedure is at best a crude approximation. The 'equilibrium melting temperature' for each thickness comes from measurements of actual melting temperatures and these values are subject to significant error. Further, in practice we should not expect the data all to lie on a single straight line but rather there should be a separate line for crystals of each thickness, due to differences in the surface free energies. Nevertheless, this technique shows that the data are best interpreted as coming from crystals growing with different

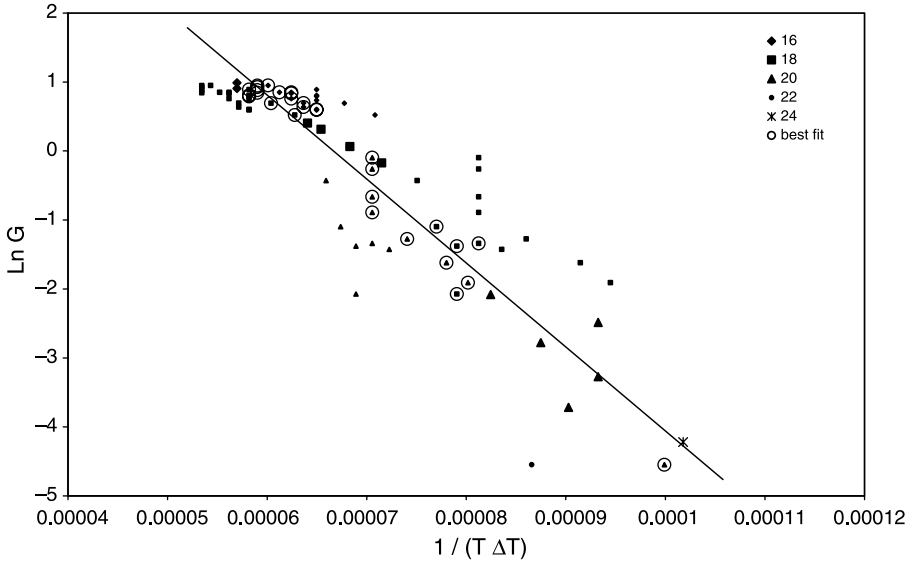

Fig. 10. Plot of $\ln G$ vs $1/T_c\Delta T$ used to deduce the most likely thickness corresponding to each growth rate. The line was constructed from the points represented by the larger symbols, where we are reasonably confident of the crystal thickness. For other points two possible values are shown, and the best fit to the line is circled.

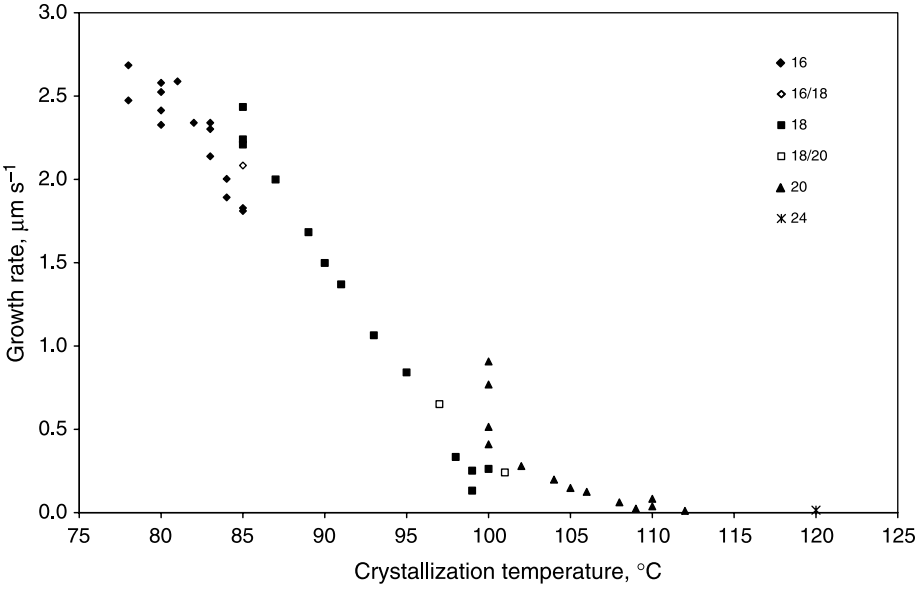

Fig. 11. Growth rate as a function of crystallization temperature, showing the most likely crystal thickness (in monomer repeat units) as deduced from Fig. 10.

thicknesses and allows us to assign a most likely thickness to each growth rate measurement. This we have done in Fig. 11, where we have replotted all the data again in the form of G vs T_c, now using different symbols to show the assumed crystal thickness of each sample. The open symbols represent points, which did not fit well to either value.

The origin of the discontinuities at 85 and 100 °C now become clear. In each case, we effectively have two superimposed curves. At 100 °C one curve (black triangles) corresponds to crystals with a thickness of 20 repeat units, and shows a sharp rise in G as ΔT increases; the other (black squares) correspond to crystals with a thickness of 18 repeat units. These crystals are at a lower effective supercooling and therefore, grow more slowly: however, nucleation of the thinner crystals is more likely to occur and they therefore, become the dominant form as the temperature is reduced further. The intermediate values are likely to arise from competition between these two competing crystal types, which may also be a factor in the particularly distorted crystal shapes that occur in this temperature range.

A similar situation is evident at 85 °C, where curves corresponding to crystals with thickness 16 (black diamonds) and 18 (black squares) repeat units are superimposed.

4.3. Spherulite morphologies

We have now established that the crystal thickness varies in a fairly continuous manner from $E/2$ to E over the temperature range studied, but that certain chain conformations are slightly more favoured than others. Furthermore, the irregular features on the growth rate vs crystallization temperature are likely to be associated with competition between two different crystal forms. From this basis, we now return to consider some aspects of the variations in spherulite morphology.

First, we note that, as already established for *n*-alkanes, the purity and monodispersity of this material does not prevent the formation of spherulites. This provides further evidence that theories of spherulite formation based on the segregation of impurities are not applicable to this system and, given the similarity in behaviour to PHB, are also unlikely to be the primary cause of spherulite growth in the polymer. Ref. [1] provides a comprehensive review of this topic.

The very distinctive band spacing obtained at crystallization temperatures of 80 °C and below is remarkably similar to that observed in PHB, despite the fact that the crystals are somewhat thinner and the chains are substantially shorter. This implies that the band spacing is linked more to the nature of the chain than to its length. However, rather than the sudden increase in band spacing seen in PHB above 90 °C, the banding in the HB 24-mer simply disappears, suggesting that a certain proportion of folds are necessary for banding to occur at all. Similar behaviour has been observed for *n*-alkanes, where banding has been reported in spherulites of $C_{294}H_{590}$ quenched rapidly from the melt but not in those grown isothermally at higher temperature [4].

Regular spherulitic growth continues up to temperatures of about 98 °C, although at the higher temperatures the growth fronts become increasingly ragged in appearance. Fig. 4(e) showed one of several examples of spherulites with very low birefringence. We do not wish to deal with these here; they will be the subject of a future publication. In brief, we believe that the low birefringence is due to a peculiar growth where the crystals grow from a cooler side of the cell towards the centre so that the optic axis moves towards the perpendicular to the slides. The actual temperature gradient across the cell and the overall growth rate allow the angle made by the optic axis to the cell to vary continuously with growth temperature so that low birefringence spherulites will grow at different crystallization temperatures depending on the precise experimental conditions. Similar variations in birefringence have been studied in PHB [14].

The change in shape of spherulites, from circular to hedritic, at the higher crystallization temperatures follows that seen both in some polymer systems and in the *n*-alkanes [1]. In general, a change to a hedritic morphology at higher crystallization temperatures has been attributed, phenomenologically, to reduced branching, possibly linked to a change in growth regime. We also note here that the most irregular crystal shapes coincide with a temperature where we believe that competition between two different stable crystal forms is occurring, so it is also conceivable that different lamellae within the aggregate are growing with different thicknesses and hence at different rates.

The change in texture towards a coarser, more fibrillar nature at higher temperatures can also be linked to the absence of branching. This has been clearly demonstrated by TEM studies of *n*-alkanes; indeed in that case spherulites do not form at all when crystals grow in the extended chain form [4]. Fig. 4(j) shows a crystal grown at 120 °C, which we believe to contain extended chains. While these crystals do have the general appearance of a spherulite, the much coarser texture and the clear linear radii produce a quite different texture to that observed at lower temperatures and suggest that branching is also greatly reduced, if not completely absent, here.

5. Conclusion

From complimentary observations of crystal morphologies, growth rates and thicknesses in oligomers of hydroxybutyrate containing 24 repeat units, grown between 10 and 120 °C, we are able to draw the following conclusions:

- Crystals can grow with a wide range of thicknesses between $E/2$ and E, where E is the extended chain length, although some thicknesses are preferred over others. This is in contrast to the long *n*-alkanes, where a clear preference for thicknesses, which are an integer fraction of the extended chain length has been observed. The difference in behaviour is likely to be due to the presence of hydrogen bonding between chain ends, which enables the oligomers to exhibit a more polymeric behaviour.
- Preferred crystal thicknesses are those which result in a relatively higher proportion of chain folds in the surface: in particular, those corresponding to $E/2$, $2/3E$, $3/4E$ and $5/6E$.
- Crystal growth rates could be measured over a wide range of crystallization temperature and pass through a maximum at 75 °C. The measurements were unusually scattered at 85 and 100 °C, and these temperatures can be linked to a change in preferred chain conformation from $2/3E$ to $3/4E$, and from $3/4E$ to $5/6E$, respectively.
- Spherulites grown below 85 °C were usually banded, with band spacings very similar to those observed in PHB.
- As the crystallization temperature was increased the banding disappeared, the shapes of the spherulites became less regular, and a coarser texture associated with reduced branching developed.

Acknowledgements

We are indebted to Professor Dieter Seebach at ETH Zurich for providing the hydroxybutyrate oligomer used in these studies. We wish to thank the ESRF for synchrotron beam time, and the EPSRC for financial support (Grant GR/R55474/01).

References

[1] Bassett DC. J Macromol Sci 2003;B42:227.
[2] Sutton SJ, Vaughan AS, Bassett DC. Polymer 1996;37:5735.
[3] Bassett DC, Olley RH, Sutton SJ, Vaughan AS. Macromolecules 1996;29:1852.
[4] Bassett DC, Olley RH, Sutton SJ, Vaughan AS. Polymer 1996;37:4993.
[5] Ungar G, Zeng X. Chem Rev 2001;101:4157 [and references therein].
[6] Li J, Organ SJ, Hobbs JK, Terry AE, Barham PJ, Seebach D. Polymer 2004;45:8913.
[7] Organ SJ, Li J, Terry AE, Hobbs JK, Barham PJ. Polymer 2004;45:8925.
[8] Li J, Organ SJ, Terry AE, Hobbs JK, Barham PJ. Polymer 2004;45:8937.
[9] Organ SJ, Ungar G, Keller A. Macromolecules 1989;22:1995.
[10] Organ SJ, Barham PJ, Hill MJ, Keller A, Morgan RL. J Polym Sci, Polym Phys Ed 1997;35:1775.
[11] Lengweiler UD, Fritz MG, Seebach D. Helv Chim Acta 1996;79:670.
[12] Barham PJ, Keller A, Otun EL, Holmes PA. J Mater Sci 1984;19:2781.
[13] Organ SJ, Barham PJ. J Mater Sci 1991;26:1368.
[14] Hobbs JK, Binger DR, Keller A, Barham PJ. J Polym Sci, Polym Phys Ed 2000;38:1575.
[15] Geil PH. J Polym Sci 1960;47:65.
[16] Bassett DC, Keller A, Mitsuhashi S. J Polym Sci A 1963;1:763.
[17] Hoffman JD, Frolen LJ, Ross GS, Lauritzen JI. J Res Natl Bur Stand A 1975;79:671.
[18] Hoffman JD. Polymer 1983;24:3.